Lead-free (Ba,Sr)TiO<inf>3</inf> – BiFeO<inf>3</inf> based multilayer ceramic capacitors with high energy density

WANG, G., LU, Z., LI, J., JI, H., YANG, H., LI, L., SUN, S., FETEIRA, Antonio <http://orcid.org/0000-0001-8151-7009>, YANG, H., ZUO, R., WANG, D. and REANEY, I.M.

Published version

WANG, G., LU, Z., LI, J., JI, H., YANG, H., LI, L., SUN, S., FETEIRA, Antonio, YANG, H., ZUO, R., WANG, D. and REANEY, I.M. (2019). Lead-free (Ba,Sr)TiO<inf>3</inf> – BiFeO<inf>3</inf> based multilayer ceramic capacitors with high energy density. Journal of the European Ceramic Society, 40 (4), 1779-1783.

Copyright and re-use policy

Lead-free $(Ba,Sr)TiO_3$ – $BiFeO_3$ based multilayer ceramic capacitors with high energy density

Ge Wang[a#], Zhilun Lu[a#], Jinglei Li[b#], Hongfen Ji[a], Huijing Yang[a], Linhao Li[a], Shikuan Sun[a], Antonio Feteira[c], Haoguang Yang[d], Ruzhong Zuo[d*], Dawei Wang[a*] and Ian M Reaney[a]

[a]Department of Materials Science and Engineering, University of Sheffield, Sheffield S1 3JD, UK.
[b]Electronic Materials Research Laboratory, Key Laboratory of the Ministry of Education and International Center for Dielectric Research, Xi'an Jiaotong University, Xi'an 710049, Shaanxi, China.
[c]Materials and Engineering Research Institute, Sheffield Hallam University, Sheffield S1 1WB, UK
[d]Institute of Electro Ceramics and Devices, School of Materials Science and Engineering, Hefei University of Technology, Hefei 230009, P. R. China.

Corresponding author: dawei.wang@sheffield.ac.uk

piezolab@hfut.edu.cn

Author contributions: Ge Wang, Zhilun Lu and Jinglei Li contributed equally to this work.

Abstract

High recoverable energy density (10 J cm^{-3}) multilayers have been fabricated from lead-free $0.61BiFeO_3$-$0.33(Ba_{0.8}Sr_{0.2})TiO_3$-$0.06La(Mg_{2/3}Nb_{1/3})O_3$ ceramics. High breakdown strength > 730 kV cm^{-1} was achieved through the optimisation of multilayer processing to produce defect-free dielectric layers 7 µm thick. Excellent temperature, frequency, fatigue stability and fast charge-discharge speed were observed in the multilayer, critical for their potential use in power electronics.

Keywords: Multilayer, Ceramic capacitor, Energy storage, Lead-free, Bismuth ferrite

Introduction

Multilayer ceramic capacitors (MLCCs) are used for pulsed power electronics due to their fast charging-discharging rate and high-power density.[1-5] The energy density (W and W_{rec}) and energy conversion efficiency (η) for dielectric capacitors are:

$$W = \int_0^{P_{max}} EdP, \quad (1)$$

$$W_{rec} = \int_{P_{rem}}^{P_{max}} EdP, \quad (2)$$

$$\eta = W_{rec}/W \quad (3)$$

where P, P_{max} and P_{rem} are the polarization, maximum polarization and remanent polarisation. Thus, high W_{rec} can be obtained by both optimising breakdown strength (E_{BDS}) and ΔP $(P_{max}-P_{rem})$. For several decades, $BaTiO_3$ (BT)-based MLCCs have been used as filters and de-couplers in electronic circuits. More recently, lead-based anti-ferroelectrics (AFEs) have been used in commercial pulsed power applications but the search for lead-free equivalents is on-going and becoming increasingly important with the rise in manufacture of electrical vehicles, where power electronics are a critical part of the engine and battery management systems. For lead-based [6-13] and lead-free ceramics, [14-45] dopants are often used to induce a phase transition from ferroelectric (FE) to anti-ferroelectrics (AFE) and relaxor-ferroelectrics (RFE) states with promising lead free ceramics reported for: BT-based [23-25]; $BiFeO_3$-$BaTiO_3$ (BF-BT)-based; [26-34] $Na_{0.5}Bi_{0.5}TiO_3$ (NBT)-based; [35-38] and $K_{0.5}Na_{0.5}NbO_3$(KNN)-based [39-42] solid solutions. These compositions not only show great potential for developing lead-free high energy density capacitors with low dissipation factor (d_f) but also exhibit considerably lower field induced strain compared to lead-based materials, [6-11] such as La doped Pb(Zr, Ti)O_3 (PLZT), an important factor in minimising mechanical failure.

In this study, we report a novel lead-free MLCC with high W_{rec} fabricated from $0.61BiFeO_3$-$0.33(Ba_{0.8}Sr_{0.2})TiO_3$-$0.06La(Mg_{2/3}Nb_{1/3})O_3$ (BF-BST-LMN) ceramics which from previous studies has been reported to have high W_{rec} ~3.38 J cm^{-3} and η ~ 59% at 230 kV cm^{-1}.[33] Optimised multilayers with a dielectric layer thickness of 7 µm revealed greatly improved W_{rec} (~ 10 J cm^{-3}) and η (~ 72%), principally due to a higher E_{BDS} (730 kV cm^{-1}).

Experimental method

$0.61BiFeO_3$-$0.33(Ba_{0.8}Sr_{0.2})TiO_3$-$0.06La(Mg_{2/3}Nb_{1/3})O_3$ ceramic calcined powder was fabricated using conventional solid-state method.[33] After ball-milling stoichiometric starting materials, mixed-powder was calcined at 800 °C for 4 h and 0.1 wt% MnO_2 was added before second ball-milling. Then the calcined powder was sieved and ball-milled with binder, plasticizer and solvent to form a slurry for tape casting. Multilayers were fabricated using an MTI MSK-AFA-II tape caster with a single doctor blade, followed by screen printed (DEK 247) Pt electrodes onto the tape. The electrode layers were laminated with the inner Pt electrode offset and hot-pressed 30 mins at 80 °C. MLCCs were sintered at 920 °C for 4 h with binder burnout at 300 °C, followed by application of a terminal Au electrode at 850 °C for 2 h.

The crystal structure of ceramic powder was studied using Bruker D2 phase X-ray diffractometer (XRD). Microstructural cross sections of MLCCs were examined using an FEI Inspect F50 scanning electron microscope (SEM) equipped with a

backscattered electron (BSE) and energy dispersive X-ray (EDX) spectroscopy detector.

Temperature-dependent dielectric permittivity and loss were examined using an Agilent 4184A precision LCR meter (Agilent Technologies Inc., Pala-Alto, CA) from room temperature (RT) to 500 °C at 1, 10, 100 and 250 kHz, respectively. Unipolar polarisation-electric field (P-E) loops of MLCCs were obtained using an aixACCT TF2000E ferroelectric tester at temperatures ranging from RT to 120 °C and frequencies ranging from 0.1 to 100 Hz. Charge-discharge behaviour of multlayers was measured using a PolyK 1801 (USA) machine. Multilayers were first charged using trek amplifier then the discharge energy was measured using a load resistor (10 kΩ) in series. An oscillator was used to collect the voltage which increases with electric field across the resistor with time. [26,27]

Results and discussion

The crystal structure of the BF-BST-LMN ceramic powder was examined using x-ray diffraction, Figure 1(a), which revealed a single perovskite phase without secondary peaks. A core-shell microstructure is observed under SEM in BSE mode, as illustrated in the inset of Figure 1(a), consistent with other reported BF-BT-based materials. [26, 27, 32, 43-45] The temperature-dependent dielectric permittivity (ε_r) and loss (*tanδ*) of BF-BST-LMN MLCCs at 1, 10, 100 and 250 kHz are presented in Figure 1(b). Similar to other reported BF-BT-based materials, including BF-BT-$Bi(Zn_{2/3}Nb_{1/3})O_3$, BF-BT-$Nd(Zr_{1/2}Zn_{1/2})O_3$ and BF-BT-$Nd(Mg_{2/3}Nb_{1/3})O_3$,[27, 32] several anomalies in ε_r were observed as a function of temperature, consistent with a core-shell microstructure due to chemical micro-segregation on slow-cooling. [26,27,32] BSE image, coupled with EDX line scan, of polished cross section of the MLCC are presented in Figure 1(c, d). The dielectric layer and electrode thickness was measured at 7 and 5 µm, respectively, with no evidence within the images of an interaction layer between ceramic and Pt.

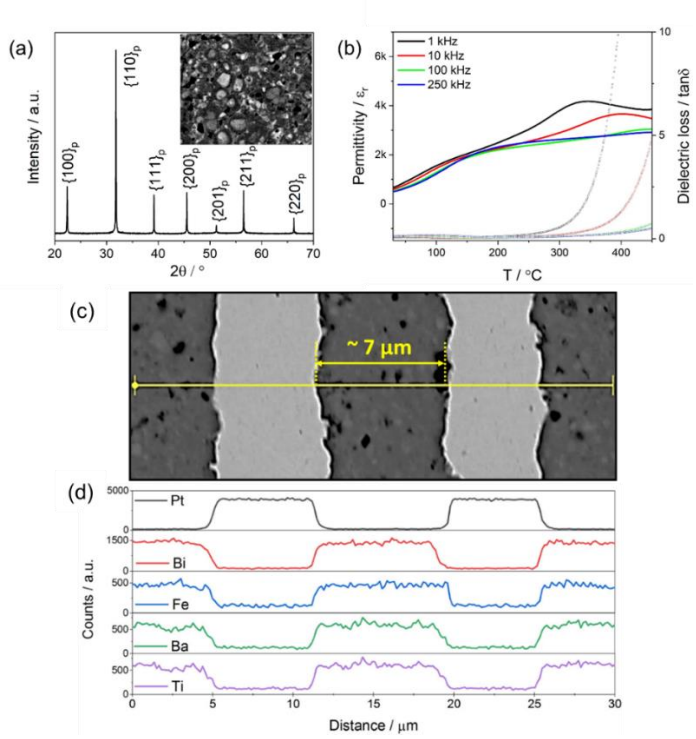

Figure 1. (a) XRD pattern of BF-BST-LMN ceramic powder; SEM microstructure of BF-BST-LMN ceramics as inset. (b) Temperature dependent permittivity and loss for BF-BST-LMN

MLCCs. (c) BSE image and (d) EDX element line scan of polished cross section of BF-BST-LMN MLCCs.

RT unipolar P-E loops of BF-BST-LMN MLCCs are shown in Figure 2(a). The E_{BDS} for multilayers increased to 730 kV cm^{-1} compared with 230 kV cm^{-1} for bulk samples due to the fabrication of thinner and defect-free dielectric layers (7 µm).[7, 12] At the highest applied electric field, P_{max} was 53 µC cm^{-2} and P_{rem} ~ 7 µC, yielding a W_{rec} ~ 10 J cm^{-3} with η ~ 72% at 730 kV cm^{-1} (Figure 2b). *In situ* temperature-dependent unipolar P-E loops of MLCCs were also obtained at 300 kV cm^{-1}, as shown in Figure 2c. The energy storage properties (W_{rec} and η) as a function of temperature (20-120°C) are displayed in Figure 2d, revealing good temperature stability (<15%).

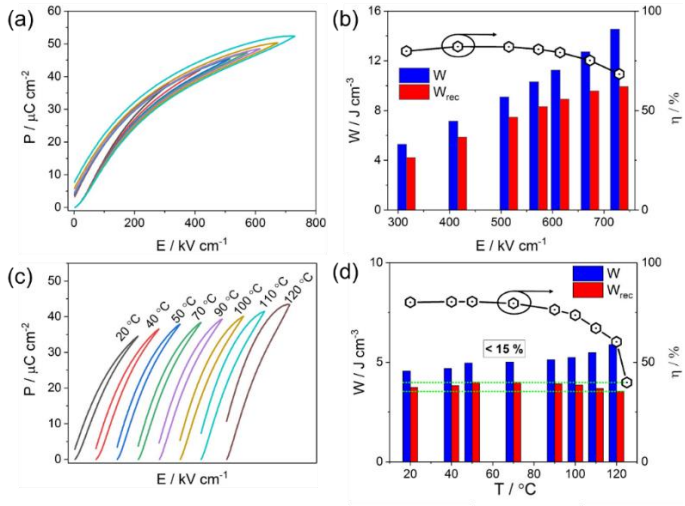

Figure 2. (a) Unipolar P-E loops and (b) Calculated energy storage properties for BF-BST-LMN MLCCs at RT; (c) Temperature dependent unipolar P-E loops and (d) calculated energy storage properties for BF-BST-LMN MLCCs as function of temperature.

Under application of the same electric field (300 kV cm^{-1}), the frequency-dependent and cycle-dependent unipolar (Figure 3) P-E loops of MLCCs were evaluated in the frequency range of 0.5 Hz to 100 Hz and up to 10^4 cycles, respectively. Frequency independence (<10%) and fatigue-resistance (<5%) were evident.

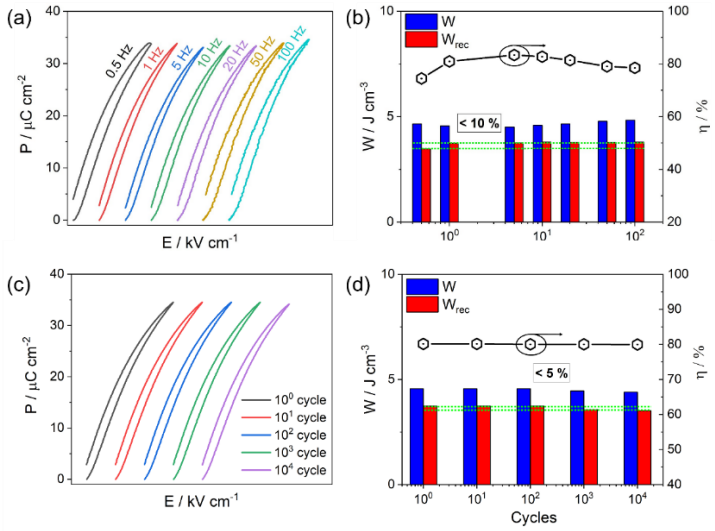

Figure 3. (a) Frequency-dependent unipolar P-E loops and (b) Calculated energy storage properties for BF-BST-LMN MLCCs as function of frequency. (c) AC cycling of unipolar P-E loops and (d) Calculated energy storage properties for BF-BST-LMN MLCCs as function of cycle number.

The charge-discharge behavior of the multilayers was investigated under different electric fields, as presented in Figure 4. The discharge processes for all applied electric fields (up to 400 kV cm^{-1}) complete within 10 μs, as shown in Figure 4a. The discharge time ($\tau_{0.9}$) is found to be 1.53 μs (Figure 4b), which is the time to discharge 90% of the total energy density (Figure 4b). The discharging energy density of multilayers as a function of electric field are displayed in Figure 4c, exhibiting a good linear relationship between the discharge energy density and the applied electric field, which is useful to the practical control application. The discharging power density of multilayers is calculated to be 2.2 MW cm^{-3} at 400 kV cm^{-1}.

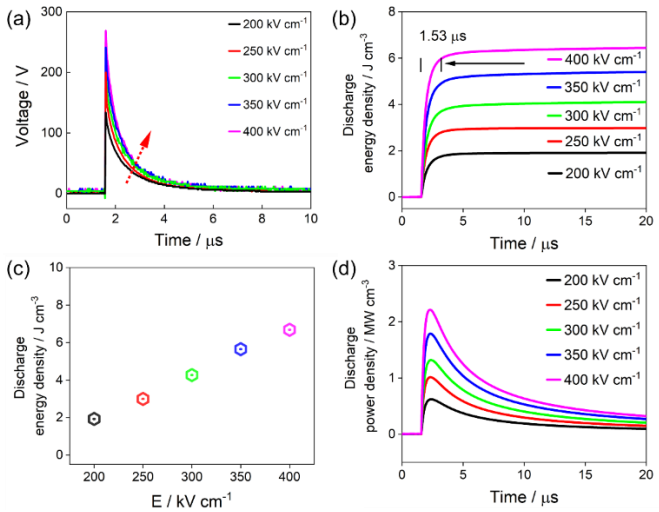

Figure 4. (a) The discharge voltage curves of MLCCs as a function of time. (b) The discharge energy density curves of MLCCs as a function of time. (c) The discharge energy density of MLCCs as a function of electric field and (d) the discharge power density of MLCCs as a function of time.

Compared with other reported lead-based/lead-free compounds (Figure 5), BF-BST-LMN multilayers deliver one of the highest known W_{rec} (~ 10 J cm^{-3}) with a fast $\tau_{0.9}$ (~1.53 μs). [23, 24, 27, 32, 35, 46-48]

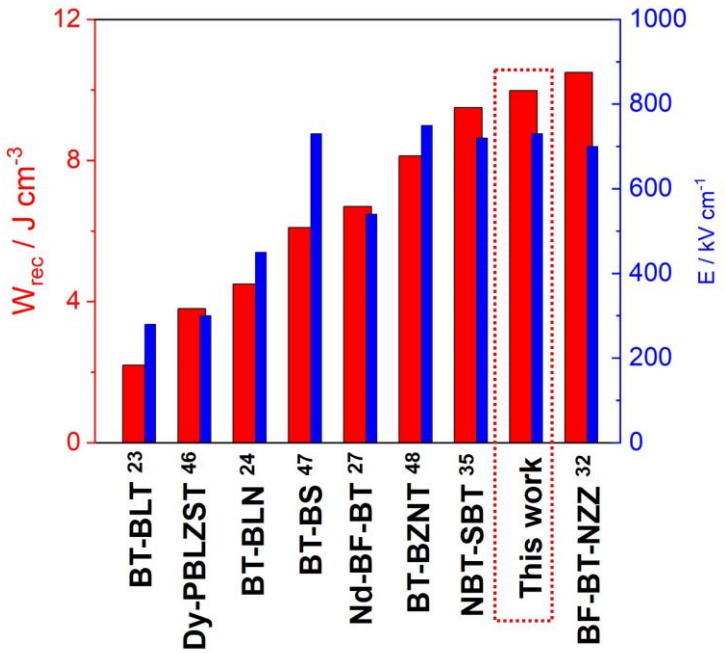

Figure 5. A comparison of W_{rec} and maximum electric field values among the recently reported lead/lead-free MLCCs at room temperature.

Conclusion

Lead-free BF-BST-LMN multilayers were fabricated with dielectric and inner Pt electrode thicknesses of 7 μm and 5 μm, respectively. The multilayers exhibited one of the highest reported values of W_{rec} ~ 10 J cm^{-1} with η ~ 72 % at 730 kV cm^{-1}. Furthermore, the MLCCs displayed good frequency stability from 0.5 Hz-100 Hz (<10%) and temperature stability from 20-120°C (<15%), fatigue-resistance up to 10^4 cycles (<5%) as well as a fast charge-discharge speed ($\tau_{0.9}$ ~1.53 μs) which are essential for practical applications.

Acknowledgements:

We thank the EPSRC for funding (Substitution and Sustainability in Functional Materials and Devices, EP/L017563/1 and Synthesizing 3D Metamaterials for RF, Microwave and THz Applications, EP/N010493/1) and support provided by Functional Materials and Devices group from University of Sheffield.

References

[1] I. Burn, D. M. Smyth, Energy storage in ceramic dielectrics, J. Mater Sci. 7 (1972) 339-343.

[2] G. R. Love, Energy Storage in Ceramic Dielectrics, J. Am Ceram Soc. 73 (1990) 323-328.

[3] C. Liu, F. Li, L. Ma, H-M. Cheng, Advanced materials for energy storage, Adv. Mater. 22 (2010) E28.

[4] H. Chen, T. Cong, W. Yang, C. Tan, T. Li, Y. Ding, Progress in electrical energy storage system: A critical review, Prog. Nat. Sci. 19 (2009) 291-312.

[5] W. Hu, Y. Liu, R. L. Wither, T. J. Frankcombe, L. Noren, A. Snashall, M. Kitchin, P. Smith, B. Gong, H. Chen, J. Schiemer, F. Brink, J. Wong-Leung, Electron-pinned defect-dipoles for high-performance colossal permittivity materials, Nat. Mater. 12 (2013) 821-826.

[6] Y. Dan, H. Xu, K. Zou, Q. Zhang, Y. Lu, G. Chang, H. Huang, Y. He, Energy storage characteristics of (Pb,La)(Zr,Sn,Ti)O_3 antiferroelectric ceramics with high Sn content, Appl. Phys. Lett. 113 (2018) 063902.

[7] F. Bian, S. Yan, C. Xu, Z. Liu, X.Chen, C. Mao, F. Cao, J. Bian, G. Wang, X. Dong, Enhanced breakdown strength and energy density of antiferroelectric Pb,La (Zr,Sn,Ti)O_3 ceramic by forming core-shell structure, J. Eur. Ceram. Soc. 38 (2018) 3170-3176.

[8] F. Zhuo, Q. Li, Y. Zhou, Y. Ji, Q. Yan, Y. Zhang, X. Xi, X. Chu, W. Cao, Large field-induced strain, giant strain memory effect, and high thermal stability energy storage in (Pb,La)(Zr,Sn,Ti)O_3 antiferroelectric single crystal, Acta Mater. 148 (2018) 28-37.

[9] J. Shen, X. Wang, T. Yang, H. Wang, J. Wei, High discharge energy density and fast release speed of (Pb, La)(Zr, Sn, Ti)O_3 antiferroelectric ceramics for pulsed capacitors, J. Alloys and compounds. 721 (2017) 191-198.

[10] X. Hao, J. Zhai, X. Yao. Improved Energy Storage Performance and Fatigue Endurance of Sr-Doped $PbZrO_3$ Antiferroelectric Thin Films, J. Am. Ceram. Soc. 92 (2009) 1133-1135.

[11] H. Zhang, X. Chen, F. Cao, G. Wang, X. Dong, Z. Hu, T. Du, Charge-Discharge Properties of an Antiferroelectric Ceramics Capacitor Under Different Electric Fields, J. Am. Ceram. Soc. 93 (2010) 4015-4017.

[12] D. Wang, M. Cao, S. Zhang, Piezoelectric properties of $PbHfO_3$-$PbTiO_3$-$Pb(Mg_{1/3}Nb_{2/3})O_3$ ternary ceramics, Phys. Status Solidi RRL. 6 (2012) 135-137.

[13] D-W. Wang, H-B. Jin, J. Yuan, B-L. Wen, Q-L. Zhao, D-Q. Zhang, M-S. Cao, Mechanical reinforcement and piezoelectric properties of PZT ceramics embedded with nano-crystalline, Chin. Phys. Lett. 27 (2010) 047701.

[14] W. Li, Z. Xu, R. Chu, P. Fu, G. Zang, Piezoelectric and dielectric properties of $(Ba_{1-x}Ca_x)(Ti_{0.95}Zr_{0.05})O_3$ lead-free ceramics, J. Am. Ceram. Soc. 93 (2010) 2942-2944.

[15] W. Li, Z. Xu, R. Chu, P. Fu, G. Zang, High piezoelectric d_{33} coefficient in $(Ba_{1-x}Ca_x)(Ti_{0.98}Zr_{0.02})O_3$ lead-free ceramics with relative high Curie temperature, Mater. Lett. 64 (2010) 2325-2327.

[16] W. Li, Z. Xu, R. Chu, P. Fu, G. Zang, Polymorphic phase transition and piezoelectric properties of $(Ba_{1-x}Ca_x)(Ti_{0.9}Zr_{0.1})O_3$ lead-free ceramics, Phys. B. 405 (2010) 4513-4516.

[17] G. Wang, D. A. Hall, Y. Li, C. A. Murray, C. C. Tang, Structural characterization of the electric field-induced ferroelectric phase in $Na_{0.5}Bi_{0.5}TiO_3$-$KNbO_3$ ceramics, J. Eur. Ceram. Soc. 36 (2016) 4015-4021.

[18] G. Wang, Z. Lu, Z. Zhang, A. Feterira, C. C. Tang, D. A. Hall, Electric field-induced irreversible relaxor to ferroelectric phase transformations in $Na_{0.5}Bi_{0.5}TiO_3$-$NaNbO_3$ ceramics, J. Am. Ceram. Soc. 102 (2019) 7746-7754.

[19] G. Wang, Y. Li, C. A. Murray, C. C. Tang, D. A. Hall, Thermally-induced phase transformations in $Na_{0.5}Bi_{0.5}TiO_3$-$KNbO_3$ ceramics, J. Am. Ceram. Soc. 100 (2017) 3293-3304.

[20] Z. Fan, C. Zhou, X. Ren, X. Tan, Domain disruption and defect accumulation during unipolar electric fatigue in a BZT-BCT ceramic, Appl. Phys. Lett. 111 (2017) 252902.

[21] Z. Fan, J. Koruza, J. Rodel, X.Tan, An ideal amplitude window again electric fatigue in BaTiO3-based lead-free piezoelectric materials, Acta Mater. 151 (2018) 253-259.

[22] Z. Fan, X. Tan, In-situ TEM study of the aging micromechanisms in a $BaTiO_3$-based lead-free piezoelectric ceramic, J. Eur. Ceram. Soc. 38 (2018) 3472-3477.

[23] W-B. Li, D. Zhou, R. Xu, D-W. Wang, J-Z. Su, L-X. Pang, W-F. Liu, G-H. Chen, $BaTiO_3$ Based Multilayers with Outstanding Energy Storage Performance for High Temperature Capacitor Applications, ACS Appl. Energy Mater. 2 (2019) 5499-5506.

[24] W-B. Li, D. Zhou, R. Xu, L-X. Pang, I. M. Reaney, $BaTiO_3$–$Bi(Li_{0.5}Ta_{0.5})O_3$ Lead-Free Ceramics and Multilayers with High Energy Storage Density and Efficiency, ACS Appl. Energy Mater. 1 (2019) 5016-5023.

[25] W-B. Li, D. Zhou, L-X. Pang, R. Xu, H-H. Guo, Novel barium titanate based capacitors with high energy density and fast discharge performance, J. Mater. Chem. A. 5 (2017) 19607-19621.

[26] D. Wang, Z. Fan, W. Li, D. Zhou, A. Feteira, G. Wang, S. Murakami, S. Sun, Q. Zhao, X. Tan, I. M. Reaney, High Energy Storage Density and Large Strain in $Bi(Zn_{2/3}Nb_{1/3})O_3$ - Doped $BiFeO_3$–$BaTiO_3$ Ceramics, ACS Appl. Energy Mater. 1 (2018) 4403-4412.

[27] D. Wang, Z. Fan, D. Zhou, A. Khesro, S. Murakami, A. Feteira, Q. Zhao, X. Tan, I. M. Reaney, Bismuth ferrite-based lead-free ceramics and multilayers with high recoverable energy density, J. Mater. Chem. A. 6 (2018) 4133-4144.

[28] T. Wang, L. Jin, T. Tian, L. Shu, Q. Hu, X. Wei, Microstructure and ferroelectric properties of Nb_2O_5-modified $BiFeO_3$-$BaTiO_3$ lead-free ceramics for energy storage, Mater. Lett. 137 (2014) 79-81.

[29] N. Liu, R. Liang, X. Zhao, C. Xu, Z. Zhou, X. Dong, Novel bismuth ferrite-based lead-free ceramics with high energy and power density, J. Am. Ceram. Soc. 101 (2018) 3259-3265.

[30] D. Zheng, R. Zuo, D. Zhang, Y. Li, Novel $BiFeO_3$-$BaTiO_3$-$Ba(Mg_{1/3}Nb_{2/3})O_3$ Lead-Free Relaxor Ferroelectric Ceramics for Energy-Storage Capacitors, J. Am. Ceram. Soc. 98 (2015) 2692-2695.

[31] D. Zheng, R. Zuo, Enhanced energy storage properties in $La(Mg_{1/2}Ti_{1/2})O_3$-modified $BiFeO_3$-$BaTiO_3$ lead-free relaxor ferroelectric ceramics within a wide temperature range, J. Eur. Ceram. Soc. 37 (2017) 413-418.

[32] G. Wang, J. Li, X. Zhang, Z. Fan, F. Yang, A. Feteira, D. Zhou, D. C. Sinclair, T. Ma, X. Tan, D. Wang, I. M. Reaney, Ultrahigh energy storage density lead-free multilayers by controlled electrical homogeneity, Energy Environ. Sci. 12 (2019) 582-588.

[33] H. Yang, H. Qi, R. Zuo, Enhanced breakdown strength and energy storage density in a new $BiFeO_3$-based ternary lead-free relaxor ferroelectric ceramic, J. Eur. Ceram. Soc. 39 (2019) 2673-2679.

[34] D. Wang, G. Wang, S. Murakami, Z. Fan, A. Feteira, D. Zhou, S. Sun, Q. Zhao, I. M. Reaney, $BiFeO_3$-$BaTiO_3$: a new generation of lead-free electroceramics, J. Adv. Dielectr. 8 (2018) 1830004.

[35] J. Li, F. Li, S. Zhang, Multilayer Lead-Free Ceramic Capacitors with Ultrahigh Energy Density and Efficiency, Adv. Mater. 30 (2018) 1802155.

[36] J. Wu, A. Mahajan, L. Riekehr, H. Zhang, B. Yang, N. Ment, Z. Zhang, H. Yan, Perovskite $Sr_x(Bi_{1-x}Na_{0.97-x}Li_{0.03})_{0.5}TiO_3$ ceramics with polar nano regions for high power energy storage, Nano Energy. 50 (2018) 723-732.

[37] F. Li, J. Zhai, B. Shen, X. Liu, H. Zeng, Simultaneously high-energy storage density and responsivity in quasi-hysteresis-free Mn-doped $Bi_{0.5}Na_{0.5}TiO_3$-$BaTiO_3$-$(Sr_{0.7}Bi_{0.2}\square_{0.1})TiO_3$ ergodic relaxor ceramics, Mater. Res. Lett. 6 (2018) 345-352.

[38] Z. Pan, D. Hu, Y. Zhang, J. Liu, B. Shen, J. Zhai, Achieving high discharge energy density and efficiency with NBT-based ceramics for application in capacitors, J. Mater. Chem. C. 7 (2019) 4072-4078.

[39] Z. Yang, H. Du, S. Qu, Y. Hou, H. Ma, J. Wang, J. Wang, X. Wei, Z. Xu, Significantly enhanced recoverable energy storage density in potassium-sodium niobate-based lead free ceramics, J. Mater. Chem. A. 4 (2016) 13778-13785.

[40] B. Qu, H. Du, Z. Yang, Q. Liu, T. Liu, Enhanced dielectric breakdown strength and energy storage density in lead-free relaxor ferroelectric ceramics prepared using transition liquid phase sintering, RSC Adv. 6 (2016) 34381-34389.

[41] T. Shao, H. Du, H. Ma, S. Qu, J. Wang, J. Wang, X. Wei, Z. Xu, Potassium-sodium niobate based lead-free ceramics: novel electrical energy storage materials, J. Mater. Chem. A. 5 (2017) 554-563.

[42] B. Qu, H. Du, Z. Yang, Q. Liu, Large recoverable energy storage density and low sintering temperature in potassium-sodium niobate-based ceramics for multilayer pulsed power capacitors, J. Am. Ceram. Soc. 100 (2017) 1517-1526.

[43] S. Murakami, D. Wang, A. Mostaed, A. Khesro, A. Feteira, D. C. Sinclair, Z. Fan, X. Tan, I. M. Reaney, High strain (0.4%) $Bi(Mg_{2/3}Nb_{1/3})O_3$-$BaTiO_3$-$BiFeO_3$ lead-free piezoelectric ceramics and multilayers, J. Am. Ceram. Soc. 101 (2018) 5428-5442.

[44] S. Murakami, N. T. A. F. Ahmed, D. Wang, A. Feteira, D. C. Sinclair, I. M. Reaney, Optimising dopants and properties in $BiMeO_3$ (Me = Al, Ga, Sc, Y, $Mg_{2/3}Nb_{1/3}$, $Zn_{2/3}Nb_{1/3}$, $Zn_{1/2}Ti_{1/2}$) lead-free $BaTiO_3$-$BiFeO_3$ based ceramics for actuator applications, J. Eur. Ceram. Soc. 38 (2018) 4220-4231.

[45] G. Wang, Z. Fan, S. Murakami, Z. Lu, D. A. Hall, D. C. Sinclair, A. Feteira, X. Tan, J. L. Jones, A. K. Kleppe, D. Wang, I. M. Reaney, Origin of the large electrostrain in $BiFeO_3$-$BaTiO_3$ based lead-free ceramics, J. Mater. Chem. A. 7(2019) 21254-21263.

[46] l. Chen, N. Sun, Y. Li, Q. Zhang, L. Zhang, X. Hao, Multifunctional antiferroelectric MLCC with high-energy- storage properties and large field-induced strain, J. Am. Ceram. Soc. 101(2018) 2313-2320.

[47] H. Ogihara, C. A. Randall, S. Trolier-McKinstry, High-Energy Density Capacitors Utilizing 0.7 $BaTiO_3$-0.3$BiScO_3$ Ceramics, J. Am. Ceram. Soc. 92 (2009) 1719-1724.

[48] Z. Cai, C. Zhu, H. Wang, P. Zhao, L. Chen, L. Li, X. Wang, High-temperature lead-free multilayer ceramic capacitors with ultrahigh energy density and efficiency fabricated via two-step sintering, J. Mater. Chem. A. 7 (2019) 14575-14582.